The Influence of Cyclometalated Ligand Motifs on the Solid-State Assemblies and Luminescent Properties of Pt(II)-Tl(I) Complexes

Sareh Paziresh,[a] Violeta Sicilia[b], Irene Ara,[a] Antonio Martín,[a] and Sara Fuertes[a]**

[a]Departamento de Química Inorgánica, Facultad de Ciencias, Instituto de Síntesis Química y Catálisis Homogénea (ISQCH), CSIC - Universidad de Zaragoza, Pedro Cerbuna 12, 50009, Zaragoza, Spain. E-mail: sfuertes@unizar.es

[b]Departamento de Química Inorgánica, Escuela de Ingeniería y Arquitectura de Zaragoza, Instituto de Síntesis Química y Catálisis Homogénea (ISQCH), CSIC - Universidad de Zaragoza, Campus Rio Ebro, Edificio Torres Quevedo, 50018, Zaragoza, Spain.

ABSTRACT

We have synthesized the HC^N_{pz} ligand, 1-(naphthalen-2-yl)-*1H*-pyrazole (**1A**), and carried out its cyclometalation reaction with [{Pt(η^3-C_4H_7)(μ-Cl)}$_2$] to give ~~the complex~~ [{Pt(Naph^N)(μ-Cl)}$_2$]. This process takes place via the intermediate [Pt(η^3-C_4H_7)Cl(HNaph^N-κN)] (**2A**) which could be isolated and fully characterized. Compound [{Pt(Naph^N)(μ-Cl)}$_2$] and the analogous N-heterocyclic carbene complex [{Pt(Naph^C*)(μ-Cl)}$_2$] (HNaph^C*-κC* = 3-methyl-1-(naphthalen-2-yl)-1*H*-imidazol-2-ylidene) were used to prepare the bis cyanide anionic derivatives N^{n}Bu$_4$[Pt(Naph^E)(CN)$_2$] (E = N_{pz} **4A**, C*$_{carbene}$ **4B**) which subsequently react with $TlPF_6$ to afford the corresponding complexes [PtTl(Naph^E)(CN)$_2$] (**5A** and **5B**). The X-ray structures of **5A** and **5B** show the presence of 2D extended networks created by organometallic "PtTl(Naph^E)(CN)$_2$" entities, each one containing a Pt→Tl dative bond (d Pt-Tl= 3.0205(3) Å **5A**, 2.9395(4) Å **5B**). These units are linked together through additional Tl···N≡C and Tl···π contacts, which in the case of **5B** renders a stair-like arrangement. NBO charge distributions analysis on ~~compounds~~ **4A** and **4B** shows a small ~~neat~~ negative charge on the Pt center for **4B** while positive for **4A**, indicating the more electron donating character of the carbene with respect to the pyrazole group. ^{195}Pt and ^{13}C NMR spectra of N^{n}Bu$_4$[Pt(Naph^E)(^{13}CN)$_2$] (E = N_{pz} **4A'**, C*$_{carbene}$ **4B'**) account for this difference. Photophysical analysis has been performed for **4A/B** and **5A/B** regarding the Naph^E fragment. The emissions of **4A** and **4B** in CH_2Cl_2 at 77 K present similar profiles and have been assigned to ^{3}ILCT [π(Naph^E) → π*(Naph^E)] excited states. The green emission of **4A** in poly(methylmethacrylate) (PMMA) film (5% wt) affords a photoluminescence quantum yield (PLQY, Φ) of 82%. In solid state, the vibronic emissions of **5A** (λmax = 528 nm) and **5B** (λmax = 561 nm) are red-shifted in relation to their precursors (λmax = 488 nm **4A**, 530 nm **4B**) and are mainly attributed to ^{3}MM′LCT [d/s σ*(Pt,Tl) → π*(Naph^E)] excited states.

INTRODUCTION

Phosphorescent square-planar platinum complexes are an active research area in the fields of biological labelling,[1,2] chemical sensing,[3,4] and light emitting devices.[5-7] The emissive behaviour of these compounds can arise from discrete molecular species, by introducing strong field ligands that raises the energy level of the radiationless d-d states and increase the quantum efficiency. To achieve this, the cyclometalated aryl-pyridine ligands are well suited systems due to their electronic features derived from the σ–donor (aryl) and π–acceptor (imine) fragments. Besides, they present synthetically-accessible modification sites within the cyclometalating skeleton that consequently vary the emitting light colour across the visible spectrum.[8-11] Likewise, the monodentate ancillary ligands L play an important role in the spectral tuning of emitted light and also in the solid-state aggregation and intermolecular interactions.[12-16] In this regard, when using non-bulky ligands the square-planar complexes can interact with each other through π–π or Pt–Pt stacking interactions which can give rise to different species of higher nuclearity (excimers or aggregates). Consequently, a change in the nature of the emissive states is produced; therefore, the $^3\pi\pi^*$ or ^{3}MMLCT excited states lead to phosphorescent red-shifted emissions in relation to those of the discrete monomer, originated from ^{3}IL/^{3}MLCT states.[17]

Many square-planar Pt(II) compounds have been proved to behave as Lewis bases to give Metal Only Lewis Pairs (MOLP) complexes featuring Pt(II)→M (M = Cu(I),[18,19] Ag(I),[20-24] Au(I),[25,26] Cd(II),[27-29] Hg(II),[30,31] Tl(I),[32-41] Pb(II)[41-43]) dative bonds. These metal–metal interactions observed in heterometallic systems have been utilised as well as a powerful tool to tune the properties of complexes by the simple modulation of distances and orientations between the units. Among the heterometallic complexes, those containing Pt^{II} – Tl^{I} dative metal–metal linkages are

versatile systems to create extended structures with functional properties such as photoluminescence ([{Pt(R-C^C*)(acac)}$_2$Tl]PF_6,[37] [TlPt($C_4H_9N_4$)$(CN)_2$],[36] "$Tl_2Pt(C_6F_5)_2(CN)_2$",[38] [TlPt(C^N)$(CN)_2$],[39]), vapochromism ([{Pt(bzq)$(C_6F_5)_2$}Tl$(Me_2CO)]_n$[41]) or mecanochromism ([{Pt(C_6F_5)(C^N)}Tl(SpyCF_3-5)]$_n$[34]). In this area, we have reported the use of anionic bis-cyanide complexes N^{n}Bu$_4$[M(C^N)$(CN)_2$] (M = Pd,[44] Pt[39]) with 7,8-benzoquinolinato (bzq) and 2-phenylpyridinato (ppy) as C^N cyclometalated ligands to create 2D-extended structures with donor–acceptor M→Tl bonds (M = Pd, Pt). Due to the presence of M-Tl bonds and the secondary interactions within the assembled network, the yellow emissions of the corresponding precursors, typically originated from ^{3}ILCT/^{3}MLCT excited states, are fairly modified and shifted to the red spectral region.

Having in mind that C,N- cyclometalated compounds with a poor π-acceptor neutral fragment like pyrazole instead of a pyridine would enlarge the energy gap and alter the emissive properties[45] and that the aryl-pyrazole platinum compounds have been barely explored,[46-52] we decided to expand the investigation to a new synthon N^{n}Bu$_4$[Pt(C^N)$(CN)_2$] (HC^N = 1-(naphthalen-2-yl)-1H-pyrazole, **4A**) whose cyclometalated skeleton (Pt(Naph^N)) also presents structural similarities with the N-heterocyclic carbene species (Pt(Naph^C*)) we have recently been investigating on.[53-56] Thus, compound N^{n}Bu$_4$[Pt(Naph^N)$(CN)_2$] (**4A)** and the counterpart, N^{n}Bu$_4$[Pt(Naph^C*)$(CN)_2$] (HC^C*-κC* = 3-methyl-1-(naphthalen-2-yl)-1*H*-imidazol-2-ylidene, **4B**) recently published by Kato and coworkers,[57] have been reacted with $TlPF_6$ to afford neutral extended structures containing Pt-Tl dative bonds, [PtTl(Naph^E)$(CN)_2$] (E = pyrazole **5A**, carbene **5B**). Structural and photophysical comparative analysis have been performed regarding the cyclometalated Pt(Naph^E) motif.

RESULTS AND DISCUSSION

Preparation of the HNaph^N ligand. One pot and stepwise strategies for cyclometalation to Pt(II).

The synthesis of the 1-(naphthalen-2-yl)-*1H*-pyrazole (HNaph^N **1A**) was accomplished by a modified Ullmann-type condensation (Scheme 1, step a and Figure S1). 2-bromonaphthalene was coupled with pyrazole in DMSO at 130ºC using copper(I) oxide and potassium carbonate. After work-up, **1A** was obtained by precipitation with *n*-hexane in good yield (*ca*. 76%). Keeping on with our developed protocol to prepare C^N- and C^C*-cyclometalated complexes of platinum(II),[58,59] the HNaph^N ligand was reacted with the dichlorido-bridged complex [{Pt(η^3-C_4H_7)(μ-Cl)}$_2$] (**Z**) (η^3-C_4H_7 = η^3-2-methylallyl) in CH_2Cl_2 to yield compound **2A** (see Scheme 1, step b and Experimental Section for details) as a pure, air-stable solid.

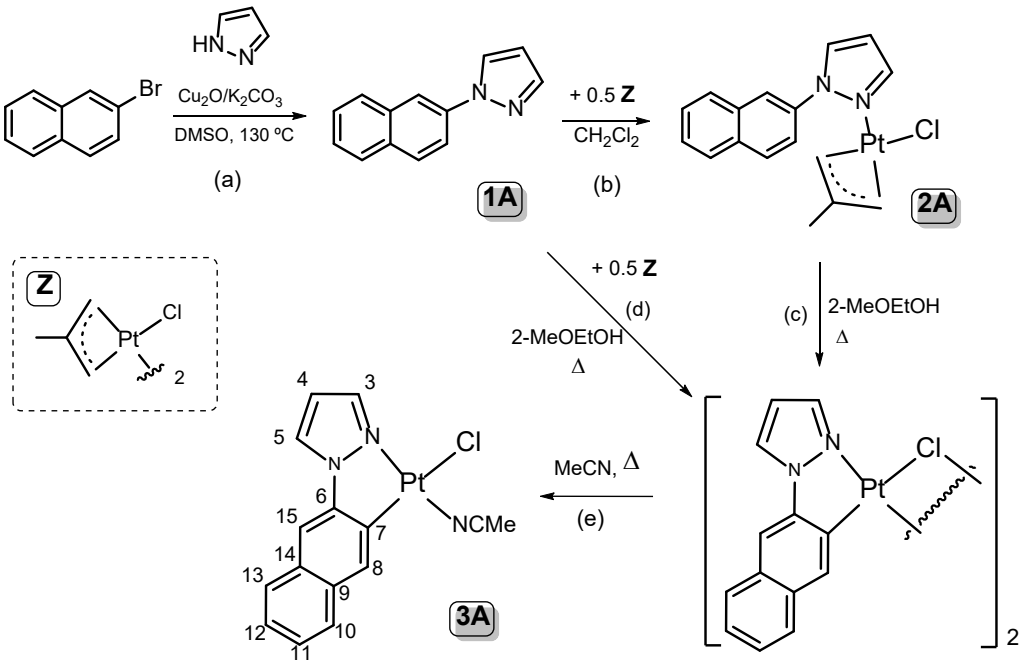

Scheme 1. Reaction pathways and Numerical Scheme for NMR spectroscopic studies

The $^{195}Pt\{^{1}H\}$ NMR spectrum shows one resonance at –4271 ppm that appears more deshielded than that obtained (^{195}Pt δ: –4457 ppm) for the analogous compound [Pt(η^3-C_4H_7)Cl(HNaph^C*-κC*)] (HNaph^C*-κC*= 3-methyl-1-(naphthalen-2-yl)-1*H*-imidazol-2-ylidene),[54] probably due to the lower basicity of the pyrazole compared to the N-heterocyclic carbene. The ^{1}H NMR spectrum in CD_2Cl_2 shows the expected signals for the HNaph^N and allyl ligands[59-61] coordinated to the Pt center in accordance with formulated structure (Figures S2-S6), which was then confirmed by single crystal X-ray diffraction (see Figure 1). The Pt-C_{allyl}, Pt-Cl and Pt-N distances are very similar to those observed in related η^3-allyl Pt(II) complexes, [Pt(η^3-C_4H_7)Cl(HC^N-κN)] (HC^N= 3,8-dinitro-6-phenylphenanthridine,[58] 2-(4-bromophenyl)imidazol[1,2-a]pyridine).[59] The naphthyl-pyrazole ligand is not planar, with the angle between the mean plane defined for each, the naphthyl (C4-C13) and the pyrazole (N1, N2, C1-C3) fragments being 57.80 (18)°.

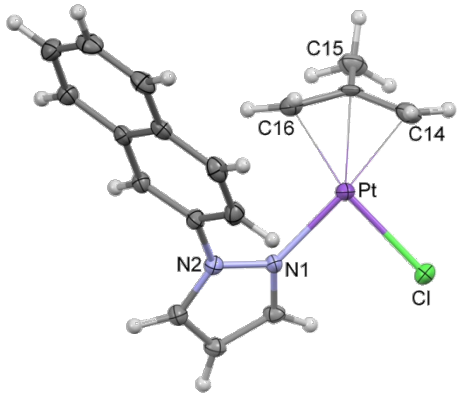

Figure 1. Molecular structure view of complex **2A**. Selected bond distances (Å) and angles (deg): Pt-N(1): 2.095(4); Pt-C(15): 2.104(5); Pt-C(14): 2.105(6); Pt-C(16): 2.111(6); Pt-Cl: 2.3570(12); N(1)-Pt-C(16): 104.2(2); C(14)-Pt-C(16): 69.5(2); N(1)-Pt-Cl: 88.11(12); C(14)-Pt-Cl: 97.97(17).

The pyrazole moiety is neither coplanar with the platinum coordination plane (Pt, Cl, N1, C14-C16), since the angle between the corresponding planes is 39.15 (16)°.

The cyclometalated chlorido-bridged compound [{Pt(Naph^N)(μ-Cl)}$_2$] could be obtained by refluxing a suspension of **2A** in 2-methoxyethanol for 4 h or through a one pot strategy, that is by refluxing a solution of the allyl complex of Pt(II), **Z**, and HNaph ^N (**1A**) in 2-methoxyethanol (see Scheme 1, steps c and d and Exptl. Section). Recrystallization of the filtered solid in boiling acetonitrile solution rendered [Pt(Naph^N)Cl(NCMe)] (**3A**) as a pure white solid in good yield (*ca*. 70%). The ^{1}H NMR spectrum was recorded in DMSO-d_6 and provides direct evidence of the purity of the prepared sample, the elimination of the allyl group, the metalation of the naphthyl moiety of the HNaph^N ligand and the presence of a molecule of acetonitrile (see Figure S7). Taking into account the well-studied reaction of chloride bridged splitting in dinuclear C,N-cyclometalated complexes[59, 62-64] and the electronic and steric characteristics of the ligands, we propose the formation of the isomer (*trans* C, Cl) for compound [Pt(Naph^N)Cl(NCMe)] (**3A**) (see scheme 1). As reported before,[54] the cyclometalation could be carried out at two nonequivalent positions of the naphthalene fragment: C15 and C7 to form two different five-membered rings, however the C-H activation took place regiospecifically at the less hindered position (C7). According to this, two singlets were observed at 8.60 and 8.21 ppm assigned to H8 and H15 respectively. Besides, the H8 proton displays Pt satellites with a Pt-H coupling constant of *ca* 50 Hz.

Synthesis and characterization of N^{n}Bu$_4$[Pt(Naph^E)(CN)$_2$]

Compound N^{n}Bu$_4$[Pt(Naph^N)(CN)$_2$] (**4A**) was prepared following the synthetic procedure already reported by us to prepare bis-cyanide compounds[16, 65] (see Scheme 2 step a, Exptl. Section and Figures S8-S12), It was fully characterized by IR, NMR, Mass spectroscopy and X-ray crystallography (see Figure 2). We also prepared N^{n}Bu$_4$[Pt(Naph^C*)(CN)$_2$] (**4B**), containing a N-heterocyclic group as the Naph^E cyclometalated fragment which was published by Kato and

co-workers very recently.[57] We have included it here for comparative purposes (see Exptl. Section and Figures S13 and S14).

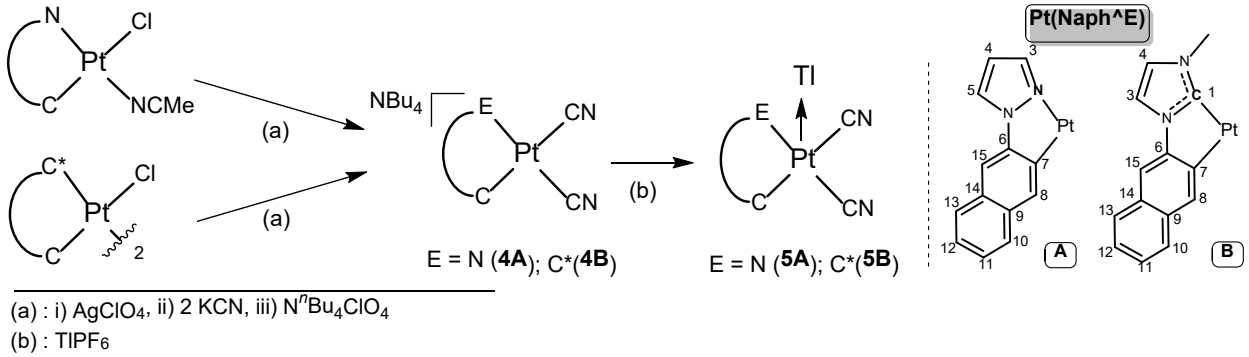

Scheme 2. Reaction pathways and numerical scheme for NMR spectroscopic studies

X-ray diffraction study on a single-crystal of **4A** shows a mononuclear anionic complex, in which the Pt atom exhibits a distorted square-planar environment due to the small bite angle of the cyclometalated ligand [N(1)-Pt-C(6) angle of 80.5(2)º] (Figure 2 left and Table S1). Bonding parameters are similar to those found in related five-membered platinacycles.[46-50] As expected, the cyanide ligand *trans* to the C_{aryl} atom features significantly longer Pt-C bond length than the other one in agreement with the stronger *trans* influence of the C_{aryl} compared to the N_{pz} donor atom [Pt-(C15) 2.028(7) vs Pt-C(16) 1.946(7) Å]. These data agree well with those observed for comparable Pt bis-cyanide complexes.[16, 66, 67] The anionic complex adopts a zig-zag arrangement in a layer, with the $N^nBu_4^+$ cations intercalated between each two layers (depicted in light grey, see Figure 2 right), thus avoiding π···π and Pt···Pt interactions among them. This repetitive motif was also observed in the analogous compounds $(N^nBu_4)[Pt(R\text{-}C\text{^}C^*)(CN)_2]$ (R = Cl, CN, CO_2Et;[65] R-C Naph **4B**[57]).

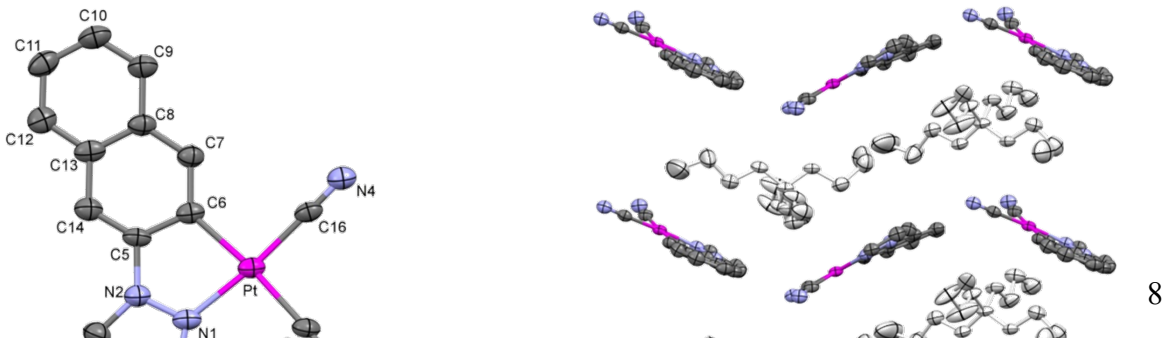

Figure 2. Left: Molecular structure view of the anion complex of **4A**. Thermal ellipsoids are drawn at the 50% probability level. Hydrogen atoms, $N^nBu_4^+$ cation and solvent molecules have been omitted for clarity. Selected bond distances (Å) and angles (deg): Pt-N(1): 2.027(6); Pt-C(6): 2.024(6); Pt-C(15): 2.028(7); Pt-C(16): 1.946(7); N(3)-C(15): 1.147(8); N(4)-C(16): 1.153(9); N(1)-Pt-C(6): 80.5(2); C(6)-Pt-C(16): 93.7(3); N(1)-Pt-C(15): 93.5(2); C(16)-Pt-C(15): 92.4(3); N(3)-C(15)-Pt: 175.7(6); N(4)-C(16)-Pt: 178.7(6). Right: Crystal packing view of **4A**

Compounds $N^nBu_4[Pt(Naph\text{^}E)(^{13}CN)_2]$ (**4A'** and **4B'**) were prepared following the same method but using $K^{13}CN$ and their $^{13}C\{^1H\}$ NMR spectra show two doublets for the two inequivalent cyanides flanked by platinum satellites (see Figures S12 and S14). As inferred from the spectroscopic data, the Pt–^{13}C coupling constants of the cyanide *trans* to the naphthyl fragment present very similar values in both compounds ($^1J_{Pt\text{-}C}$ = 856.5 Hz **4A'**, $^1J_{Pt\text{-}C}$ = 828.0 Hz **4B'**). However, that corresponding to the cyanide *trans* to five-membered ring is considerably larger in **4A'** ($^1J_{Pt\text{-}C}$ = 1445.3 Hz) than in **4B'** ($^1J_{Pt\text{-}C}$ = 1043.0 Hz) which is in agreement with the higher trans influence of the carbenic atom (C*) compared to N_{pz}.

The $^{195}Pt\{^1H\}$ NMR spectrum of **4A** shows a singlet at –4180 ppm that appears less shielded than that of **4B** (δPt = –4481 ppm, see Figure S15). This is in accordance with the more electron donating character of the carbene group in relation to that of the pyrazole ring. To confirm this, NBO charge distribution analyses were performed on **4A** and **4B** at the DFT/M06/SDD/6-31G*

level of theory in solution of dichloromethane. As a result of the four σ-C atoms bonded to the platinum center and the anionic nature, the atomic charge on the Pt center of carbene derivative (**4B**) presents a negative value (–0.111), whereas that of **4A** still keeps a positive atomic charge of ~ +0.023. Thus, this follows the tendency of the ^{195}Pt chemical shifts, and it can be explained in terms of the bigger donor ability of C^C* with respect to C^N ligand, in part due to the lower electronegativity of the C atom with respect to the N atom. Analogous results were found in other bis cyanide anionic compounds when comparing the C^N-(benzoquinolate and 2-phenylpyridinate) and C^C*- cycloplatinated fragments.[65]

Synthesis and characterization of new Pt-Tl building blocks for 2D extended solids

Treatment of $N^nBu_4[Pt(Naph^E)(CN)_2]$ (E = N_{pz} **4A**, $C^*_{carbene}$ **4B**) with the equimolar amount of $TlPF_6$ in methanol rendered the compounds $[PtTl(Naph^E)(CN)_2]$ (**5A**, **5B**) as pale yellow solids in good yields (see Exptl. Section and Scheme 2 step b). The most significant feature of the IR spectra is the presence of two ν (C≡N) (2123, 2111 cm^{-1} **5A**; 2124, 2109 cm^{-1} **5B**) absorptions according to the *cis* arrangement of the cyanide ligands.[16]

Crystal structures of compounds **5A** and **5B** appear in Figures 3, 4 and S16 and selected bond distances and angles are listed in Table 1. As can be seen, these compounds generate extended networks formed by organometallic "$PtTl(Naph^E)(CN)_2$" units, each one containing a donor–acceptor Pt(II)–Tl(I) bond, which are connected through additional contacts. The molecular structures reveal a square-based pyramid environment around the platinum center with the thallium atom being located in the apical position. The Pt–Tl bond distances [**5A**: 3.0205(3) Å; **5B**: 2.9395(4) Å] are comparable to those reported in related systems containing donor–acceptor

Pt(II)–Tl(I) bonds[34-37, 39, 40, 68] and consequently, the Pt–Tl vector is basically perpendicular to the coordination plane of the Pt(II) center [angle with the normal: 6.33(1)º (**5A**), 5.84(12)º (**5B**)].

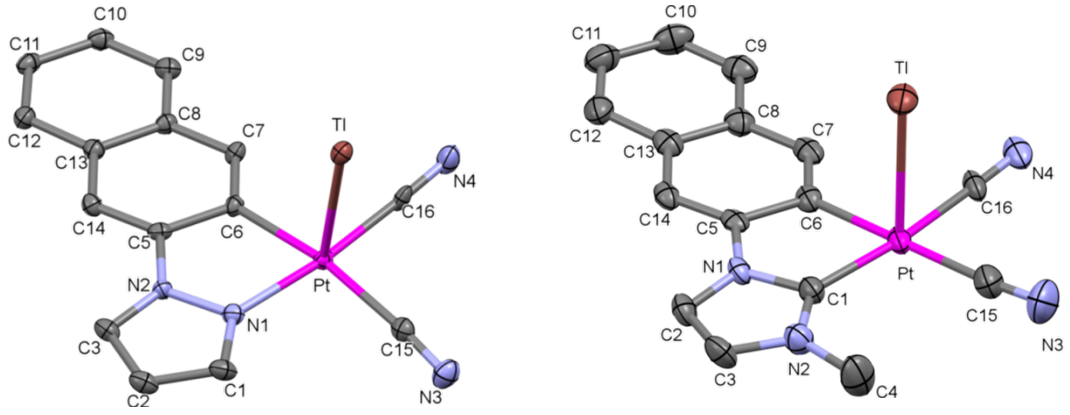

Figure 3. Molecular structure view of complexes **5A** (left) and **5B** (right). Hydrogen atoms and solvent molecules have been omitted for clarity.

In both complexes, the base of the pyramid consist of "Pt(Naph^E)$(CN)_2$" units with the platinum center exhibiting a distorted square-planar environment due to the small bite angle of the Naph^E-cyclometalated group (*ca*. 80°). The Pt-C and Pt-N distances are comparable to those observed in other platinum complexes with C^C*,[53-55, 69] C^N_{pz}[46, 48-50] and cyanide ligands.[16, 36, 39, 66, 67, 70] It is worth noting that the Pt-C(16) distance in **5A** (1.945 Å) is slightly smaller than that in **5B** (1.984 Å) due to minor *trans* influence of the N_{pz} in relation to the $C_{carbene}$ one. In-depth inspection of the crystal packing arrangement shows different 2D extended networks for the Pt/Tl complexes.

Table 1. Selected bond lengths (Å) and angles (deg) for compounds **5A** and **5B**

	5A (E**=N(1))**	**5B (**E**=C(1))**
Pt-Tl	3.0205 (3)	2.9395(4)
Pt-E	2.023 (4)	2.018 (7)
Pt-C(6)	2.034 (4)	2.052 (7)
Pt-C(15)	2.028 (5)	2.030 (9)
Pt-C(16)	1.946 (5)	1.984 (7)
Tl-N(4)#1	2.730 (4)	2.676 (7)
Tl-N(4)#2		2.715 (7)
N(3)-C(15)	1.150 (6)	1.144 (11)
N(4)-C(16)	1.158 (6)	1.144(9)
Tl-Tl#2	3.7677(4)	
C(6)-Pt-C(16)	94.09 (18)	92.1 (3)
C(16)-Pt-C(15)	92.30(19)	88.2 (3)
C(15)-Pt-E	93.58 (17)	99.7 (3)
E-Pt-C(6)	80.26 (17)	80.0 (3)
N(4)#1-Tl-N(4)#2		74.8 (2)
N(4)#1-Tl-Pt	92.61 (10)	95.61 (13)
N(4)#2-Tl-Pt		95.62 (13)
C(16)-N(4)-Tl#3		117.7 (6)
C(16)-N(4)-Tl#2		136.6 (6)
C(16)-N(4)-Tl#4	138.2(4)	
N(4)-C(16)-Pt	177.9 (4)	178.5 (7)
N(3)-C(15)-Pt	173.9 (4)	174.2 (8)

Symmetry elements used to generate equivalent atoms for **5A**: #1 x,y+1,z #2 -x,-y+1,-z+1 #3 -x,y,-z+1/2 #4 x,y-1,z

Symmetry transformations used to generate equivalent atoms: for **5B:** #1 x,y+1,z #2 -x+1/2,-y-1/2,-z+1 #3 x,y-1,z

In **5A** each thallium center in addition to the Pt-Tl bond is interacting with three nitrogen atoms from three "PtTl(Naph^E)$(CN)_2$" units and completes its electronic requirements with an oxygen atom from a water molecule of crystallisation exhibiting a distorted square-based pyramidal environment. The existence of the water molecule must be due to the use of non anhydrous solvents. The platinum atom is located at the apical position with angles close to 90 degrees (green dashed lines in Figure 4,top) and the Pt–Tl line forms an angle with the normal to the coordination plane of the Tl(I) center of 6.33(1)º. In **5B**, the thallium center is connected to two nitrogen atoms from two "PtTl(Naph^E)$(CN)_2$" units within the same layer and fulfills its electronic demands through Tl–π (arene) contacts (3.287–3.475 Å) with the naphthyl moiety from another adjacent unit generating a stair-like structure (Figure 4 bottom and S16). These Tl–π (arene) separations are within the range for the reported ones in this type of extended structures.[39, 40, 71] Also, on a closer examination of the contacts within the same layer, we can observe the self-association of "PtTl(Naph^C*)$(CN)_2$" pairs through two Tl−N(4)−C(16)−Pt bridges shaping eight-membered cycles (see Figure 4 bottom) identical to those formed in [MTl(bzq)$(CN)_2$] (bzq= 7,8-benzoquinolinate; M = Pt,[39] Pd[44]). Additionally, this pair joins to another from the adjacent layer through a double Tl···N bridge (see inset of Figure 4 bottom, red dotted line) with distances 2.676 (7) and 2.715 (7) Å. All the Tl···N (2.676 – 2.968 Å) and Tl···O (2.945 Å) separations in crystal structures of **5A** and **5B** are longer than those corresponding for covalent bonds but shorter than the sum of the covalent radii of Tl^I (1.55 Å) and the van der Waals radii of N (1.55 Å) and O (1.52 Å);[72] these separations are comparable to those found in related derivatives, such as [PtTl(C^N)$(CN)_2$] (C^N= 7,8-benzoquinolinate (bzq), 2-phenylpyridinate (ppy)) or [{PtTl(bzq)$(CC\text{-}C_5H_4N\text{-}2)_2\}_2$],[39] [*trans,trans,trans*-$Tl_2\{Pt(C_6F_5)_2(CN)_2\}(CH_3COCH_3)_2]_n$.[38] and [{Pt(R-C^C*)(acac)$\}_2$Tl]PF_6.[37]

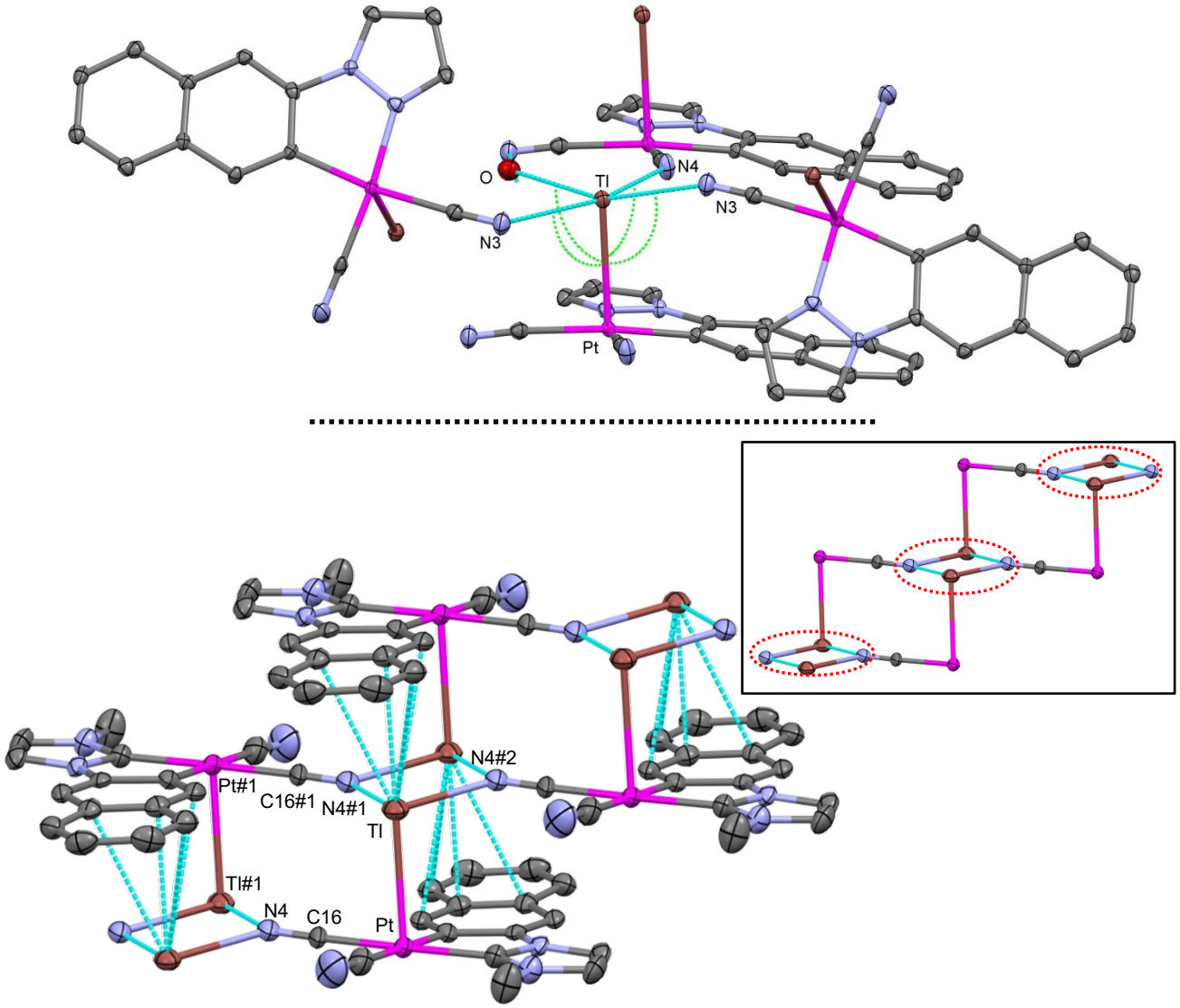

Figure 4. Supramolecular structure views of complexes **5A** (top) and **5B** (bottom). Hydrogen atoms and solvent molecules have been omitted for clarity. Inset: Schematic view.

Given the more electron donating character of the Naph^C* ligand compared to Naph^N_{pz} and the consequent negative charge on the Pt center calculated by NBO analysis, the donor–acceptor Pt–Tl bond distance in **5B** is shorter than the observed in **5A**. Also, the N4 of the cyanide *trans* to the carbene (**5B**) seems to be more basic than the one trans to the pyrazole (**5A**). In **5B**, N4 is able to

interact with two different Tl^+ centers at the same time with fairly short distances whereas in **5A** it just interacts with one Tl^+, showing no stair-like arrangement in the extended lattice (see Figure 4).

Due to the low solubility of complexes **5A** and **5B** in other common organic solvents, the NMR spectra were registered in DMSO (see Figure S17). The ^1H NMR signals corresponding to the cyclometalated Naph^E fragment are equal to those of the precursors (**4A** and **4B**), which suggest the complete dissociation of the Pt-Tl bimetallic unit in solution of DMSO (see Figure S18 for **4B/5B**) but undoubtedly shows the purity of the sample with no traces of the $N^nBu_4^+$ cation.

Optical properties and DFT/TD-DFT calculations

*Absorption spectra and DFT calculations for **4A**.* Absorption data are summarized in Table S2 and Figures 5 and S19, S20). A solution of **4A** in CH_2Cl_2 shows strong absorption bands in the high energy (HE) region at $\lambda < 300$ nm ($\varepsilon > 10^4$ M^{-1} cm^{-1}), commonly assigned to singlet intraligand (^{1}IL) transitions of the cyclometalated C^N ligand.[12, 16, 58, 59, 66] Additionally it displays an intense low-energy absorption at $\lambda \sim 320$ nm ($\varepsilon \approx 10^4$ M^{-1} cm^{-1}) and the lowest-energy one at $\lambda \sim 358$ nm ($\varepsilon \approx 10^3$ M^{-1} cm^{-1}). The absorption bands of $N^nBu_4[Pt(Naph^N)(CN)_2]$ (**4A**) are almost identical but slightly red shifted when compared to those of the counterpart **4B**.[57] A concentration dependence study in CH_2Cl_2 (see Figure S19) revealed that the lowest-energy absorption band follows Beer's law in the concentration range from 5×10^{-6} to 10^{-3} M, suggesting that no remarkable ground-state aggregation occurs within this range.

DFT and TD-DFT calculations in solution of CH_2Cl_2 for **4A** have been carried out to provide correct assignments for the UV-vis absorptions. The optimized geometries of the ground state, S_0, were carried out at the B3LYP/SDD(Pt)/6-31G*(ligands atoms) level (Table S3). The calculated S_1 transition in CH_2Cl_2 is in agreement with the experimentally observed absorption (Figure 5)

and it arises from HOMO→LUMO (75%) with minor contributions of H-1→L (12%) and H→L+1 (8 %) transitions.

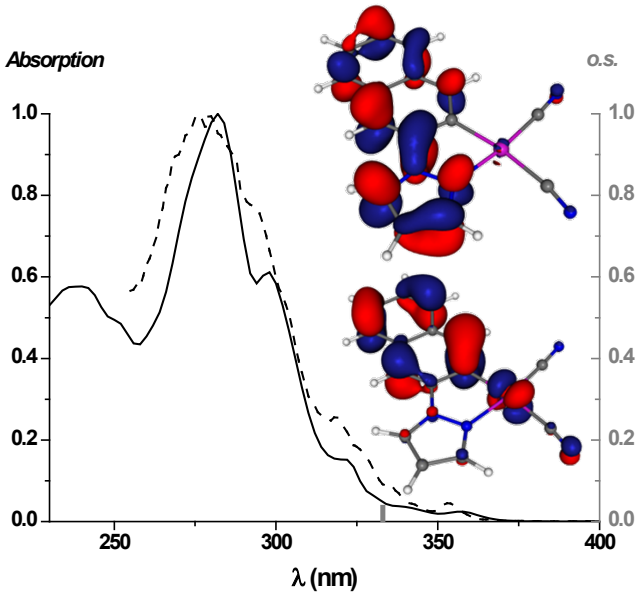

Figure 5. Normalized UV−vis absorption (—, 298 K) and excitation (---, 77 K) spectra of **4A** in CH_2Cl_2 and S_1 calculated transition for **4A** in CH_2Cl_2 (grey bar). Pictures of the HOMO (bottom) and LUMO (top) for **4A**.

As depicted in Figure 5, the highest occupied molecular orbital (HOMO) is mainly centered on the naphthyl group (82%) and to a minor extent on the Pt center (14%). By contrast, the lowest unoccupied molecular orbital (LUMO) is constructed from orbitals located on the naphthyl group (60%) and the pyrazole fragment (37%). Therefore, the lowest energy transition can be attributed to a ^{1}ILCT [π(Naph^N) → π*(Naph^N)] transition with some contribution of ^{1}MLCT [5d(Pt) → π*(Naph^N)]. Due to the great insolubility of the Pt/Tl compounds (**5A** and **5B**) in common and non-coordinating organic solvents at rt, it was not possible to carry out the photophysical study (absorption and emission spectra) in solution, even at low concentrations (10^{-5} M).

*Emission spectra of **4A/B** and **5A/B***. The emission spectra of **4A** in different rigid media [solid state, rigid matrix of CH_2Cl_2 at 77 K and PMMA films at 5% wt] are almost identical ~~between each other~~. They show highly structured green emissions at λ_{max} = 488 nm with vibronic spacings of 1407 and 1447 cm^{-1} corresponding to the C=C/C=N stretches of the cyclometalated Naph^N ligand (see Figure 6 and Table 2) and long monoexponential decay times (τ up to 581 μs).

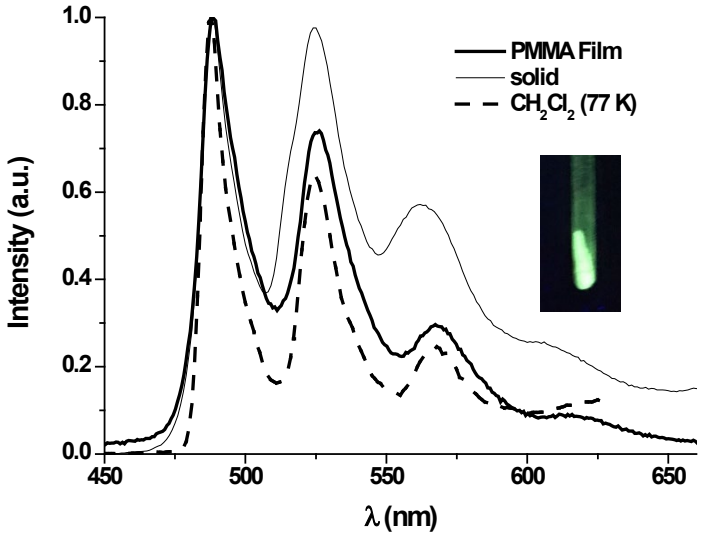

Figure 6. Normalized emission spectra of **4A**. Picture taken under UV light (λex = 365 nm).

Considering as well that the excitation spectrum exhibits identical profile to the corresponding UV−vis absorption one (see Figure 5) and the TD-DFT calculations, these phosphorescent emissions must be mostly due to ^{3}ILCT [π(Naph^N) $\rightarrow$ π^*(Naph^N)] states of the monomeric species. In PMMA film (5% wt) under Ar atmosphere **4A** affords a particularly high photoluminescent quantum yield reaching up to 82%. As far as we know, it is the highest value recorded for C^N-pyrazole-based Pt(II) complexes at rt.[46, 50-52] The emission of **4B** in diluted rigid

media was reported in EtOH-MeOH by Kato et al.,[57] and appears within the same spectral region. Our measurement of **4B** in CH_2Cl_2 (10^{-5} M, 77 K) gave an analogous shaped emission to that of **4A** but with the maximum slightly blue-shifted (472 nm, Table 2 Figure S21). This is in agreement with the findings we reported recently,[65] in which the carbenic fragment enlarges the HOMO LUMO gap in the C^C* complexes and shifts the emission to the blue region.

Table 2. Photophysical data.

Comp	Media (T/K)	λ_{ex} (nm)	λ_{em} (nm)	τ (μs)[c]	ϕ[d] (%)
4A	CH_2Cl_2[a, b](77)	355	488_{max}, 524, 567	581	
	PMMA (298)	355	488_{max}, 524, 567		82
	Solid (298)	360	488_{max}, 524, 564	84	7
4B	CH_2Cl_2[a](77)	350	472_{max}, 510, 546, 592_{sh}	466	
	Solid (298)[57]		530_{max}, 572, 621	69	72
	Solid (77)[57]		525_{max}, 570, 620	77	73
5A	Solid (298)	365	528_{max}, 570, 617	44.7	4
	Solid (77)	350	527_{max}, 572, 620_{sh}	59.2	
5B	Solid (298)	370	561_{max}, 603, 660_{sh}	22	40
		500	561_{sh}, 603_{sh}, 665_{max}	1.1	
	Solid (77)	370	555_{max}, 603, 656_{sh}	25	
		470	555_{sh}, 603_{sh}, 665_{max}	1.3	

a = 10^{-5} M; *b* = 10^{-3} M; *c*= measurements at λ_{max}; *d* = 5 % wt PMMA films in Ar atmosphere

The emissive behaviour of the Pt–Tl complexes was only registered in powdered solid samples due to the insolubility in non-coordinating organic solvents. Upon excitation at λ~ 370 nm, powdered samples of **5A** and **5B** at r.t. show structured bands at 528 and 561 nm, respectively, with vibronic separations of 1241 – 1546 cm^{-1} (Figure 7) similar to those observed in the starting compounds, yet significantly red-shifted in relation to them (**4A** and **4B**, see Table 2). Similar behaviour was previously observed for $[MTl(C^N)(CN)_2]$ (C^N= bzq, ppy; M = Pd,[44] Pt[39]) and $[PtTl(bzq)(C{\equiv}CR)_2]$ (R = Ph, C_5H_4N-2)[39] which was attributed to the raised energy of the HOMO due to the presence of the M–Tl bonds. Therefore, considering all this along with the vibronic pattern and the rather long decays of the emissions, they have been tentatively attributed to a

transition from a metal-metal'-to-ligand charge transfer ^{3}MM'LCT [d/s σ*(Pt,Tl) → π*(Naph^E)] excited state with some intraligand ^{3}IL [π(Naph^E) → π*(Naph^E)] character.

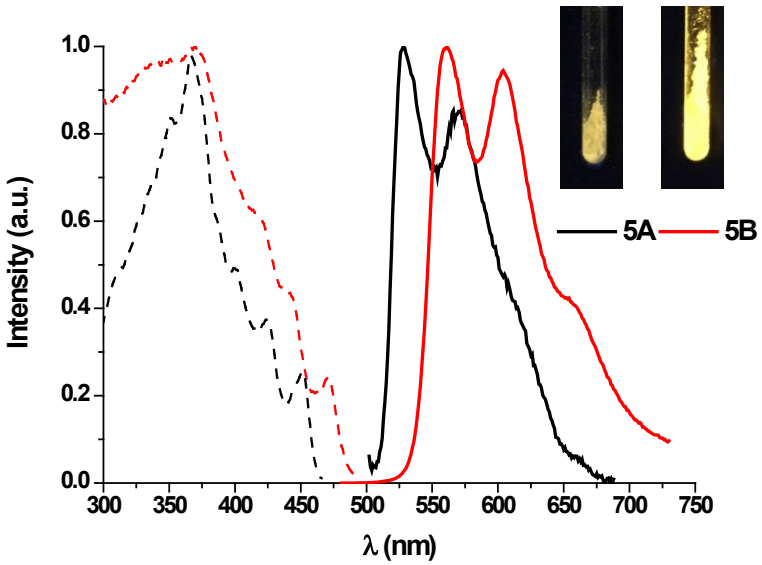

.

Figure 7. Normalized excitation (---) and emission (—) spectra of **5A** and **5B** in solid state at rt. Pictures taken at 365 nm.

Different from the trend observed for **4A** and **4B** in CH_2Cl_2 (10^{-5}M) (see Figure 6 and Table 2), in this case, the emission of **5B** appears red shifted when compared to that of **5A** (Figure 7). Thus, in view of the shorter Pt-Tl bond in **5B** (2.9395(4) Å) with respect to that in **5A** (3.0205(3) Å), it seems that the more electron donating character of the carbene fragment strengthens the Pt-Tl bond, raising the energy of the HOMO [d/s σ*(Pt,Tl)] and therefore decreasing the HOMO-LUMO gap compared to that in [PtTl(Naph^N)$(CN)_2$](**5A**). This structural and spectroscopic relationship was also observed in the counterpart complexes [PtTl(bzq)$(C{\equiv}C\text{-}C_5H_4N\text{-}2)_2$] and [PtTl(C^N)$(CN)_2$] (C^N= bzq, ppy).[39] From their emission spectra at 77 K and the X-ray data, it

can be inferred that those compounds with shorter Pt-Tl distances rendered emissions more shifted to the red than those with longer Pt-Tl bond lengths.[39] Finally, as observed in related complexes,[37] the QY values of the compounds containing $Pt^{II} \rightarrow Tl^{I}$ dative bonds are lower than the corresponding starting materials but still very high for **5B** (40%), even better than those reported in the literature.[34, 35, 41] It is worth mentioning that only **5B** displays a wavelength dependent emissive behaviour at rt and 77 K (Figure 8 for rt ~~and S22~~). Upon excitation at 500 nm, the emission profile changes, whereby a weaker and structureless band appears at λ_{max} = 665 nm along with the remaining contribution of the HE band. This low-energy band displays a shorter lifetime measurement (~ 1.1 μs) it is presumably attributed to $^{3}\pi\pi^{*}$ excited states. Therefore, the dual emission has been observed in many occasions and is likely due to a relatively slow internal conversion between two close lying emissive states (^{3}MM´LCT/$^{3}\pi\pi^{*}$).[34,39,73]

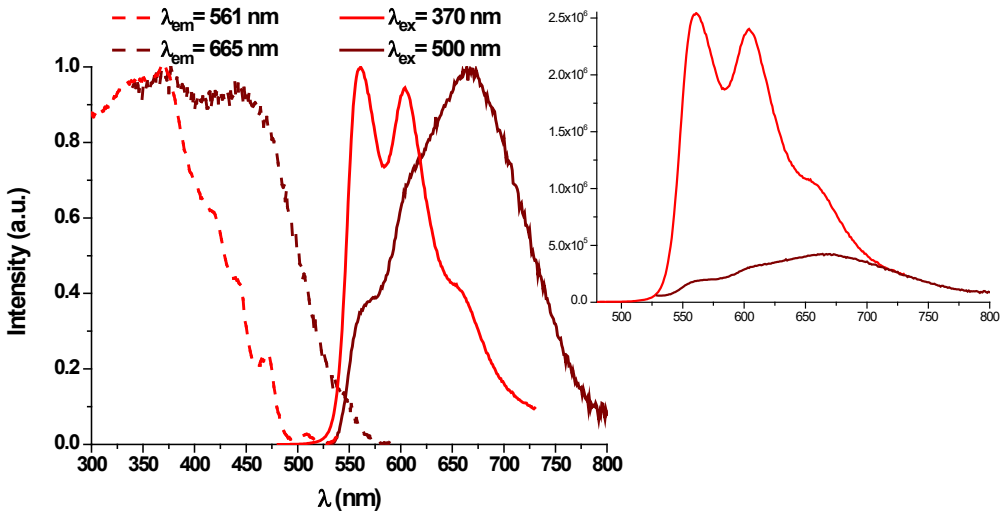

Figure 8. Normalized excitation and emission spectra of **5B** in solid state at 298 K. Inset: Unnormalized emission spectra

CONCLUSIONS

Anionic bis-cyanide complexes $N^nBu_4[Pt(Naph\text{^}E)(CN)_2]$ containing a cyclometalated naphthyl moiety bearing different neutral fragments (pyrazol **4A**, carbene **4B**) have been prepared following our step-wise protocol starting from the ligand synthesis up to the cyloplatinated systems. Again, this proves the success of using complex $[\{Pt(\eta^3\text{-}C_4H_7)(\mu\text{-}Cl)\}_2]$ to perform the cyclometalation reactions. Compounds **4A** and **4B** were used as synthons by reacting with $TlPF_6$ to construct self-organized networks, such as $\{PtTl(Naph\text{^}E)(CN)_2\}_n$ (E = N_{pz} **5A**, $C_{carbene}$ **5B**). These units containing a Pt→Tl dative bond within the same entity are linked together through additional Tl···N≡C and Tl···π contacts between adjacent ones giving birth to different extended structures. The more electron donating character of the carbene group with respect to the pyrazole one was confirmed by NBO charge distributions analysis on compounds **4A** and **4B** which shows for **4B** a small ~~neat~~ negative charge on the Pt center**.** This influences not only the ^{195}Pt NMR data but also the electronic features of the platinum center, with the Pt–Tl bond distance being shorter in **5B**, and the assembly ability of the $\{PtTl(Naph\text{^}E)(CN)_2\}$ units. It also affects the emissive behavior of **4B**/ **5B** with respect to that of **4A** /**5A**. In this sense, this study delivers that the carbenic fragment enlarges the HOMO LUMO gap in the Naph^C*-Pt discrete complexes and shifts the ^{3}ILCT emission to the blue region in relation to that of the Naph^N-Pt ones. However, in the metal-metal bonded Pt-Tl complexes, the emission mainly arises from ^{3}MM'LCT [d/s σ*(Pt,Tl) → π*(Naph^E)] excited states and is more shifted to the red spectral region in complex bearing the carbenic fragment **5B**, which exhibits the shorter Pt-Tl bond.

EXPERIMENTAL SECTION

General procedures and instrumentation. ^{1}H, $^{13}C\{^1H\}$ and $^{195}Pt\{^1H\}$ NMR spectra were recorded on a Bruker Avance 400 MHz instrument using the standard references: $SiMe_4$ (^{1}H and ^{13}C), and Na_2PtCl_6 in D_2O (^{195}Pt). Chemical shifts, δ, and coupling constants, *J* are given in ppm

and Hz, respectively and assignments are based on ^{1}H-^{1}H COSY and ^{1}H-^{13}C HSQC and HMBC experiments. Infrared spectra were recorded on Perkin-Elmer Spectrum 100 FT-IR spectrometer (ATR range 250-4000 cm^{-1}) as neat solids. Mass spectra were acquired using the Microflex matrix-assisted laser desorption ionization-time-of-flight (MALDI-TOF) Bruker or an Autoflex III MALDI-TOF Bruker instruments. C, H, and N analyses were carried out in a Perkin-Elmer 2400 CHNS analyzer. UV-visible spectra were registered on a Unicam UV4 spectrophotometer. Steady-state photoluminescence spectra were recorded on a Jobin-Yvon Horiba Fluorolog FL-3-11 Tau 3 spectrofluorimeter. Phosphorescence lifetimes were recorded with a Fluoromax phosphorimeter accessory containing a UV xenon flash tube. Nanosecond lifetimes were recorded with a Datastation HUB-B with a nanoLED controller and software DAS6. The lifetime data were fitted using the Jobin-Yvon software package and the Origin Pro 8 program. Quantum yields in solid and in PMMA film were measured using the Hamamatsu Absolute PL Quantum Yield Measurement System C11347-11. PMMA films were prepared by drop casting solutions of the complex (10^{-2} M, 5% weight) and PMMA in 0.5 mL of dichloromethane onto optical grade quartz plates. All chemicals were used as supplied and [{Pt(η^3-C_4H_7)(μ-Cl)}$_2$] (**Z**)[60,61] and [{Pt(Naph^C*)(μ-Cl)}$_2$][54] were prepared following the literature procedures. $TlPF_6$ **Caution!** Thallium salts are highly toxic when ingested, inhaled, or absorbed through the skin. They should be handled with extreme caution. Solvents are non-anhydrous unless stated otherwise.

1-(2-naphthalenyl)-*1H*-pyrazole (HNaph^N) (1A).

A reaction mixture of 2-bromonaphthalene (0.67 g, 3.23 mmol), pyrazole (0.336 g, 4.93 mmol), Cu_2O (0.046 g, 0.32 mmol), K_2CO_3 (0.894 g, 6.4 mmol) and DMSO (6 mL) was stirred at 130 ˚C under Ar atmosphere for 2 days. Ethyl acetate (60 mL) was added to the cooled mixture at r.t. and filtered through Celites. The resulting solution was washed with water (80 mL), and then brine (20

mL). The organic layer was dried over $MgSO_4$, and evaporated to dryness. The addition of n-hexane (5 mL) to the residue gave a white solid (0.476 g, 75.8%). ^{1}H NMR (400 MHz, DMSO-*d*$_6$): δ= 8.65 (1H, d, $^3J_{H,H}$ = 2.3, H_{pz}), 8.35 (1H, br s, H_{Naph}), 8.07 (2H, m, H_{Naph}), 7.97 (2H, m, H_{Naph}), 7.81 (1H, d, $^3J_{H,H}$ = 1.1, H_{pz}), 7.55 (2H, m, H_{Naph}), 6.61 (1H, dd, $^3J_{H,H}$ = 2.3, $^3J_{H,H}$ = 1.1, H_{pz}).

[Pt(η^3-C_4H_7)Cl(HNaph^N-κN)] (2A). Compound **1A** (0.083 g, 0.42 mmol) was added to a stirred solution of [{Pt(η^3-C_4H_7)(μ-Cl)}$_2$] (0.123 g, 0.21 mmol) in CH_2Cl_2 (6 mL) at r.t. After 1h, the solution was evaporated to dryness and n-hexane (5 mL) was added to the residue to give a pale yellow solid, **2A** (0.124 g, 60%). Found: C, 42.31; H, 3.82; N, 5.73. Calc. for $C_{17}H_{17}ClN_2Pt$: C, 42.55; H, 3.57; N, 5.84. IR (cm^{-1}): ν = 292 (m, Pt-Cl). MS (MALDI+): m/z 441.1 [M-Cl]$^+$. ^{1}H NMR (400 MHz, CD_2Cl_2): δ= 8.18 (1H, dd, $^3J_{3,4}$ = 2.3, $^4J_{3,5}$ = 0.8, $^3J_{3,Pt}$ = 11.7, H_3), 8.13 (1H, d, $^3J_{15,7}$ = 1.7, H_{15}), 7.92-7.99 (4H, m, $H_{5,\,8,\,10,\,13}$), 7.86 (1H, dd, $^3J_{7,8}$ = 8.7, $^4J_{7,15}$ = 1.5, H_7), 7.61 (2H, m, $H_{11,\,12}$), 6.67 (1H, t, $^3J_{H,H}$ = 2.4, H_4), 3.37 (1H, m, $^2J_{Pt\text{-}H}$ = 29.4, $H_{syn,}$ η^3-C_4H_7), 2.70 (1H, m, $^2J_{Pt\text{-}H}$ = 35.0, $H_{syn,}$ η^3-C_4H_7), 1.89 (1H, m, $^2J_{Pt\text{-}H}$ = 74.0, $H_{anti,}$ η^3-C_4H_7), 1.62 (3H, s, $^3J_{Pt\text{-}H}$ = 80.9, Me, η^3-C_4H_7), 1.23 (1H, m, $^2J_{Pt\text{-}H}$ = 81.2, $H_{anti,}$ η^3-C_4H_7). ^{13}C{^{1}H} NMR plus HMBC and HSQC (100.6 MHz, CD_2Cl_2): δ = 143.3 (s, $^2J_{C\text{-}Pt}$ = 27.2, C_3), 136.9 (s, C_6), 132.9 (s, C_5), 132.7 (s, $C_{9,\,14}$), 129.1 (s, C_8), 128.1, 127.9 (s, 2C, $C_{10,13}$), 127.4, 127.3 (s, 2C, $C_{11,12}$), 123.6, (s, C_{15}), 123.3 (s, C_7), 111.9 (s, $C^{2'}$, η^3-2-Me-C_3H_4), 108.0 (s, $^3J_{C\text{-}Pt}$ = 32.9, C_4), 44.4 (s, $^1J_{C\text{-}Pt}$ = 258.8, $C^{1'}$, η^3-2-Me-C_3H_4), 39.8 (s, $^1J_{C\text{-}Pt}$ = 257.4, $C^{3'}$, η^3-2-Me-C_3H_4), 21.8 (s, $^2J_{C\text{-}Pt}$ = 52.0, $C^{4'}$ (Me), η^3-2-Me-C_3H_4). ^{195}Pt{H} NMR (86 MHz, CD_2Cl_2): δ= –4271 (s). Single crystals of **2A** were obtained by slow diffusion of diethyl ether into saturated CH_2Cl_2 solutions.

[Pt(Naph^N)Cl(NCMe)] (3A). Method 1. Compound **1A** (0.450 g, 2.31 mmol) was added to an orange solution of [{Pt(η^3-C_4H_7)(μ-Cl)}$_2$] (0.660 g, 1.15 mmol) in 2-methoxyethanol (8 mL). After

stirring the mixture for 1 h at r.t., it was refluxed for 4 hours and then allowed to reach room temperature. The resulting dark grey precipitate was filtered off and washed with CH_2Cl_2 (5 mL) and Et_2O (5 mL) to afford [{Pt(Naph^N)(μ-Cl)}$_2$] as a grey solid. The resulting solid was recrystallized by dissolving in 60 mL of boiling CH_3CN including carbon activated, filtering through Celite and washing with CH_3CN (3 x 5 mL). The solution was evaporated to dryness and diethyl ether (10 mL) was added to give **3A** as a white solid (0.679 g, 69.3%). **Method 2.** A suspension of **2A** (0.075 g, 0.15 mmol) in 2-methoxyethanol (10 mL) was refluxed for 4 h, to give a dark grey solid, which was filtered and washed with CH_2Cl_2 (3 mL) and Et_2O (5 mL) and identified as [{Pt(Naph^N)(μ-Cl)}$_2$]. The solid was recrystallized following the purification step described in method 1 (0.024g, 20%). Found: C, 38.48; H, 2.30; N, 8.47. Calcd for $C_{15}H_{12}ClN_3Pt$: C, 38.76; H, 2.60; N, 9.04. IR (cm^{-1}): ν = 267 (m, Pt-Cl). ^{1}H NMR (400 MHz, DMSO-d_6): δ= 9.05 (1H, dd, $^3J_{3\text{-}4}$ = 2.9, $^4J_{3\text{-}5}$ = 0.6, H_3), 8.60 (1H, s, $^3J_{8\text{-}Pt}$ = 50.1, H_8), 8.26 (1H, dd, $^3J_{5\text{-}4}$ = 2.4, $^4J_{3\text{-}5}$ = 0.5, H_5), 8.20 (1H, s, H_{15}), 7.81 and 7.73 (2H, d, $^3J_{H\text{-}H}$ = 8.0, H_{10} and H_{13}), 7.50-7.41 (2H, m, H_{11} and H_{12}), 6.90 (1H, t, $^3J_{H\text{-}H}$ = 2.6, H_4), 2.07 (3H, s, free MeCN).

N^{n}Bu$_4$[Pt(Naph^N)(CN)$_2$] (4A). KCN (32.0 mg, 0.49 mmol) was added to a freshly prepared suspension of [Pt(Naph^N)(NCMe)$_2$]ClO_4 (0.245 mmol) in MeOH (15 mL) at r.t (obtained by reaction of **3A** (111.5 mg, 0.24 mmol) with $AgClO_4$ (50.0 mg, 0.24 mmol) in acetonitrile). After 2 hours the solvent was evaporated to a volume of *c.a.* 5 mL and cooled in the freezer for 10 minutes. It was then filtered through celite and washed with 2 x 5 mL of cold MeOH (-30 ºC). The solution was evaporated to dryness, the residue was suspended in 30 mL of acetone and treated with N^{n}Bu$_4ClO_4$ (82.2 mg, 0.24 mmol). After 2 hours the solvent was removed under reduced pressure, the residue was then washed with 5 mL H_2O and the solid was filtered and washed with 2 x 5 mL H_2O. After 2 hours in the oven (96 ºC), the residue was recrystallized from CH_2Cl_2/*n*-

hexane to give **4A** as colorless crystals. Yield: 60 mg, 35%. Anal. Calcd (%) for $C_{31}H_{45}N_5Pt$: C 54.53, H 6.64, N 10.26. Found: C 53.91, H 6.32, N 10.32. IR (cm^{-1}): ν = 2122, 2112 (m, CN). MS (MALDI-): m/z 440.1 [M-N^{n}Bu$_4$]$^-$. ^{1}H NMR (400 MHz, CD_2Cl_2): δ = 8.43 (1H, s, $^3J_{8\text{-Pt}}$ = 55.0, H_8), 8.15 (2H, d, $^3J_{H\text{-}H}$ = 2.5, H_3 and H_5), 7.71-7.83 (2H, m, H_{10} and H_{13}), 7.63 (1H, s, H_{15}), 7.34-7.40 (2H, m, H_{11} and H_{12}), 6.56 (1H, t, $^3J_{H\text{-}H}$ = 2.5, H_4), 3.24 (m, 8H, CH_2, N^{n}Bu$_4^+$), 1.62 (m, 8H, CH_2, N^{n}Bu$_4^+$), 1.39 (m, 8H, CH_2, N^{n}Bu$_4^+$), 0.94 (t, $^3J_{H\text{-}H}$ = 7.3, 12H, CH_3, N^{n}Bu$_4^+$). ^{13}C{^{1}H} NMR plus HMBC and HSQC (101 MHz, CD_2Cl_2): δ = 144.32 (s, C_7), 142.3 (s, C_3), 137.7 (s, C_8), 133.3 (s, C_6), 131.0 (s, C_9, C_{14}), 127.3, 127.3 (s, C_{10} and C_{13}), 126.1 (s, C_5), 125.1, 124.8 (s, C_{11} and C_{12}), 108.1 (s, C_4), 107.3 (s, C_{15}), 59.1 (s, CH_2, N^{n}Bu$_4^+$), 24.0 (s, CH_2, N^{n}Bu$_4^+$), 19.6 (s, CH_2, N^{n}Bu$_4^+$), 13.3 (s, CH_3, N^{n}Bu$_4^+$). ^{195}Pt{^{1}H} NMR (85.6 MHz, CD_2Cl_2): δ = -4180.9. **N^{n}Bu$_4$[Pt(Naph^N)(^{13}CN)$_2$] (4A')** was prepared following the method described for **4A**, but using K^{13}CN. ν_{max}/cm^{-1} 2075, 2066 (^{13}C≡N). ^{13}C{^{1}H} NMR (101 MHz, CD_2Cl_2): δ = 137.6 (d, $^2J_{C\text{-}C}$ = 4.8, $^1J_{Pt\text{-}C}$ = 856.5, $^{13}CN_{trans\text{-}C}$), 115.2 (d, $^2J_{C\text{-}C}$ = 4.8, $^1J_{Pt\text{-}C}$ = 1445.3, $^{13}CN_{trans\text{-}N}$). Single crystals of **4A** were obtained by slow diffusion of *n*-hexane into saturated CH_2Cl_2 solutions.

N^{n}Bu$_4$[Pt(Naph^C*)(CN)$_2$] (4B). Compound **4B** was recently published.[57] We report here our synthesis method following a similar procedure to **4A**, by using [{Pt(Naph^C*)(μ-Cl)}$_2$] (0.122 g, 0.14 mmol), $AgClO_4$ (0.058 g, 0.28 mmol), KCN (0.036 g, 0.56 mmol) and N^{n}Bu$_4$ClO$_4$ (0.090 g, 0.26 mmol). **4B** was obtained as a white solid (0.108 g, 57%). Found: C, 53.66; H, 6.93; N, 9.64. Calcd (%) for $C_{32}H_{47}N_5Pt\cdot H_2O$: C, 53.77; H, 6.91; N, 9.80. IR (cm^{-1}): ν = 2120, 2107 (m, CN). MS (MALDI-): m/z 453.9 [M-N^{n}Bu$_4$]$^-$. ^{1}H NMR (400 MHz, CD_2Cl_2): δ = 8.56 (1H, s, $^3J_{8\text{-Pt}}$ = 57.7, H_8), 7.77- 7.68 (2H, m, H_{10} and H_{13}), 7.45 (1H, d, $^3J_{3\text{-}4}$ = 2.0, H_3), 7.40 (1H, s, $^4J_{Pt\text{-}15}$ = 9.5, H_{15}), 7.31 (2H, m, H_{11} and H_{12}), 6.92 (1H, d, H_4), 4.15 (3H, s, Me, C^C*), 3.21 (8H, m, CH_2, N^{n}Bu$_4^+$), 1.59 (8H, m, CH_2, N^{n}Bu$_4^+$), 1.37 (8H, m, CH_2, N^{n}Bu$_4^+$), 0.93 (12H, t, $^3J_{H\text{-}H}$ = 7.3, CH_3, N^{n}Bu$_4^+$).

$^{13}C\{^1H\}$ NMR plus HMBC and HSQC (101 MHz, CD_2Cl_2): δ = 172.7 (s, C_1), 148.4 (s, C_6), 142.9 (s, C_7), 139.3 (s, $^2J_{Pt\text{-}C8}$ = 60.8, C_8), 134.0 (s, C_9), 132.0 (s, C_{14}), 127.8, 127.7 (s, C_{10} and C_{13}), 125.1, 124.9 (s, C_{11} and C_{12}), 122.6 (s, $^3J_{Pt\text{-}C4}$ = 27.8, C_4), 115.0 (s, $^3J_{Pt\text{-}C3}$ = 37.2, C_3), 106.8 (s, $^3J_{Pt\text{-}C15}$ = 22.2, C_{15}), 59.5 (s, CH_2, $N^nBu_4^+$), 39.4 (s, $^3J_{Pt\text{-}C}$ = 20.8, Me, C^C*), 24.6 (s, CH_2, $N^nBu_4^+$), 20.2 (s, CH_2, $N^nBu_4^+$), 14.0 (s, CH_3, NBu_4^+). $^{195}Pt\{^1H\}$ NMR (64.3 MHz, CD_2Cl_2): δ = -4481.2.

N^nBu_4[Pt(Naph^C*)(^{13}CN)$_2$] (4B') was prepared following the method described for **4B**, but using $K^{13}CN$. ν_{max}/cm^{-1} 2073, 2061 ($^{13}C{\equiv}N$). $^{13}C\{^1H\}$ NMR (101 MHz, CD_2Cl_2): δ = 136.9 (d, $^2J_{C\text{-}C}$ = 5.7, $^1J_{Pt\text{-}C}$ = 828, $^{13}CN_{trans\text{-}Caryl}$), 135.2 (d, $^1J_{Pt\text{-}C}$ = 1043, $^{13}CN_{trans\text{-}C*}$).

Synthesis of [PtTl(Naph^N)(CN)$_2$] (5A). A solution of **4A** (50 mg, 0.07 mmol) in methanol (5 mL) is treated with $TlPF_6$ (24 mg, 0.07 mmol). After stirring at r.t. for 3 hours the resulting suspension was filtered and washed with MeOH (3 mL) and Et_2O (5 mL) and dried to render a pale yellow solid, **5A**. Yield: 40 mg, 88%. Found: C, 27.68; H, 1.47; N, 8.44. Calcd (%) for $C_{15}H_9N_4PtTl$: C, 27.94; H, 1.41; N, 8.69. IR (cm^{-1}): ν = 2123, 2111 (m, CN). ^1H NMR (300 MHz, DMSO-*d*$_6$): δ = 8.88 (1H, d, $^3J_{H\text{-}H}$ = 2.7, H_{pz}), 8.24 (1H, s, $^3J_{8\text{-}Pt}$ = 53.1, H_8), 8.08 (1H, s, H_{15}), 8.01 (1H, d, $^3J_{H\text{-}H}$= 2.2, H_{pz}), 7.75 (2H, m, H_{10} and H_{13}), 7.38 (2H, m, H_{11} and H_{12}), 6.76 (1H, t, H_4). Suitable crystals of **5A** were obtained by slow diffusion of diethyl ether into saturated DMSO solutions.

Synthesis of [PtTl(Naph^C*)(CN)$_2$] (5B). A solution of **4B** (0.100 g, 0.14 mmol) in methanol (10 mL) is treated with $TlPF_6$ (0.050 g, 0.14 mmol). After stirring at r.t. for 1 hour the resulting suspension was filtered and washed with MeOH (3 mL) and Et_2O (5 mL) and dried to render a pale yellow solid, **5B** (0.080 g, 85%). Found: C, 28.91; H, 1.75; N, 8.33. Calcd (%) for $C_{16}H_{11}N_4PtTl$: C, 29.17; H, 1.68; N, 8.57. IR (cm^{-1}): ν = 2124, 2109 (m, CN). ^1H NMR (400 MHz,

DMSO-d_6): δ = 8.38 (1H, s, $^3J_{8\text{-Pt}}$ = 57.3, H_8), 8.04 (1H, d, $^3J_{3\text{-}4}$ = 2.0, 1H, H_3),7.74 (1H, s, $^4J_{\text{Pt-}15}$= 8.5 , H_{15}), 7.69- 7.66 (2H, m, H_{10} and H_{13}), 7.39 (1H, d, H_4), 7.33-7.30 (2H, m, H_{11} and H_{12}), 4.06 (3H, s, Me, C^C*). Suitable crystals of **5B** were obtained by slow diffusion of methanol into saturated DMSO solutions.

ASSOCIATED CONTENT

Supporting Information.

The Supporting Information is available free of charge on the ACS Publications website.

Crystallographic and computational details; NMR spectra; X-ray crystallographic data and structures; theoretical calculations; UV-Vis and emission spectra (PDF); Crystallographic data (CIF); Cartesian coordinates (XYZ)

Accession Codes

CCDC 1921181−1921184 contain the supplementary crystallographic data for this paper.

AUTHOR INFORMATION

Corresponding Author

*Email: sfuertes@unizar.es

*Email: sicilia@unizar.es

ACKNOWLEDGMENTS

This work was supported by the Spanish Ministerio de Ciencia, Innovación y Universidades/FEDER (Project PGC2018-094749-B-I00), the Gobierno de Aragón (Grupo E17_17R) and Feder 2014-2020 (Construyendo Europa desde Aragón). S. P. thanks the Iran National Science Foundation and the Shiraz University Research Council for Grants nº. 95844501 and 93038832. The authors thank the Centro de Supercomputación de Galicia (CESGA) for

generous allocation of computational resources.provided financial support for this project. The authors declare no competing financial interests

References

1. Mauro, M.; Aliprandi, A.; Septiadi, D.; Kehr, N. S.; De Cola, L., When Self-Assembly Meets Biology: Luminescent Platinum Complexes for Imaging Applications. *Chem. Soc. Rev.* **2014**, *43*, 4144-4166.
2. Ma, D. L.; He, H. Z.; Leung, K. H.; Chan, D. S. H.; Leung, C. H., Bioactive Luminescent Transition-Metal Complexes for Biomedical Applications. *Angew. Chem. Int. Ed.* **2013**, *52*, 7666-7682.
3. Wenger, O. S., Vapochromism in Organometallic and Coordination Complexes: Chemical Sensors for Volatile Organic Compounds. *Chem. Rev.* **2013**, *113*, 3686-3733.
4. Zhao, Q.; Li, F.; Huang, C., Phosphorescent Chemosensors Based on Heavy-Metal Complexes. *Chem. Soc. Rev.* **2010**, *39*, 3007-3030.
5. Fleetham, T.; Li, G. J.; Li, J., Phosphorescent Pt(II) and Pd(II) Complexes for Efficient, High-Color-Quality, and Stable OLEDs. *Adv. Mater.* **2017**, *29*, 1601861.
6. Cebrián, C.; Mauro, M., Recent Advances in Phosphorescent Platinum Complexes for Organic Light-Emitting Diodes. *Beilstein J. Org. Chem.* **2018**, *14*, 1459-1481.
7. Yam, V. W. W.; Au, V. K. M.; Leung, S. Y. L., Light-Emitting Self-Assembled Materials Based on d(8) and d(10) Transition Metal Complexes. *Chem. Rev.* **2015,** *115*, 7589-7728.
8. Farley, S. J.; Rochester, D. L.; Thompson, A. L.; Howard, J. A. K.; Williams, J. A. G., Controlling Emission Energy, Self-Quenching, and Excimer Formation in Highly Luminescent NΛCΛN-Coordinated Platinum(II) Complexes. *Inorg. Chem.* **2005**, *44*, 9690-9703.
9. Ebina, M.; Kobayashi, A.; Ogawa, T.; Yoshida, M.; Kato, M., Impact of a Carboxyl Group on a Cyclometalated Ligand: Hydrogen-Bond- and Coordination-Driven Self-Assembly of a Luminescent Platinum(II) Complex. *Inorg. Chem.* **2015**, *54*, 8878-8880.
10. Stacey, O. J.; Platts, J. A.; Coles, S. J.; Horton, P. N.; Pope, S. J. A., Phosphorescent, Cyclometalated Cinchophen-Derived Platinum Complexes: Syntheses, Structures, and Electronic Properties. *Inorg. Chem.* **2015**, *54*, 6528-6536.
11. Bossi, A.; Rausch, A. F.; Leitl, M. J.; Czerwieniec, R.; Whited, M. T.; Djurovich, P. I.; Yersin, H.; Thompson, M. E., Photophysical Properties of Cyclometalated Pt(II) Complexes: Counterintuitive Blue Shift in Emission with an Expanded Ligand π System. *Inorg. Chem.* **2013**, *52*, 12403-12415.
12. Díez, A.; Forniés, J.; Fuertes, S.; Lalinde, E.; Larraz, C.; López, J. A.; Martín, A.; Moreno, M. T.; Sicilia, V., Synthesis and Luminescence of Cyclometalated Compounds with Nitrile and Isocyanide Ligands. *Organometallics* **2009**, *28*, 1705-1718.
13. Rossi, E.; Colombo, A.; Dragonetti, C.; Roberto, D.; Demartin, F.; Cocchi, M.; Brulatti, P.; Fattori, V.; Williams, J. A. G., From Red to Near Infra-Red OLEDs: the Remarkable Effect of Changing from X = –Cl to –NCS in a Cyclometallated [Pt(NΛCΛN)X] Complex {NΛCΛN = 5-mesityl-1,3-di-(2-pyridyl)benzene}. *Chem. Commun.* **2012,** *48*, 3182-3184.
14. Chen, Y.; Li, K.; Lu, W.; Chui, S. S. Y.; Ma, C. W.; Che, C. M., Photoresponsive Supramolecular Organometallic Nanosheets Induced by $Pt^{II}\cdots Pt^{II}$ and C-H$\cdots\pi$ Interactions. *Angew. Chem. Int. Ed.* **2009**, *48*, 9909-9913.
15. Forniés, J.; Sicilia, V.; Borja, P.; Casas, J. M.; Díez, A.; Lalinde, E.; Larraz, C.; Martín, A.; Moreno, M. T., Luminescent Benzoquinolate-Isocyanide Platinum(II) Complexes: Effect of

Pt···Pt and π···π Interactions on their Photophysical Properties. *Chem. Asian J.* **2012**, *7*, 2813-2823.
16. Forniés, J.; Fuertes, S.; López, J. A.; Martín, A.; Sicilia, V., New Water Soluble and Luminescent Platinum(II) Compounds, Vapochromic Behavior of $[K(H_2O)][Pt(bzq)(CN)_2]$, new Examples of the Influence of the Counterion on the Photophysical Properties of d(8) Square-Planar Complexes. *Inorg. Chem.* **2008**, *47*, 7166-7176.
17. Aliprandi, A.; Genovese, D.; Mauro, M.; De Cola, L., Recent Advances in Phosphorescent Pt(II) Complexes Featuring Metallophilic Interactions: Properties and Applications. *Chem. Lett.* **2015**, *44*, 1152-1169.
18. Moret, M. E.; Serra, D.; Bach, A.; Chen, P., Transmetalation Supported by a Pt^{II}-Cu^{I} Bond. *Angew. Chem. Int. Ed.* **2010**, *49*, 2873-2877.
19. Yin, G. Q.; Wei, Q. H.; Zhang, L. Y.; Chen, Z. N., Luminescent Pt^{II}-M^{I} (M = Cu, Ag, Au) Heteronuclear Alkynyl Complexes Prepared by Reaction of $[Pt(C{\equiv}CR)_4]^{2-}$ with $[M_2(dppm)_2]^{2+}$ (dppm = Bis(diphenylphosphino)methane). *Organometallics* **2006,** *25*, 580-587.
20. Usón, R.; Forniés, J.; Tomas, M.; Casas, J. M.; Cotton, F. A.; Falvello, L. R., New Compounds with Platinum to Silver Bonds Unsupported by Covalent Bridges. *J. Am. Chem. Soc.* **1985**, *107*, 2556-2557.
21. Yamaguchi, T.; Yamaguchizaki, F.; Ito, T., A Helical Metal−Metal Bonded Chain via the Pt→Ag Dative Bond. *J. Am. Chem. Soc.* **2001**, *123*, 743-744.
22. Janzen, D. E.; Mehne, L. F.; VanDerveer, D. G.; Grant, G. J., Cationic Five-Coordinate Pt^{II} Complexes as Donors in the Formation of Pt→Ag Dative Bonds. *Inorg Chem* **2005**, *44*, 8182-8184.
23. Jamali, S.; Mazloomi, Z.; Nabavizadeh, S. M.; Milic, D.; Kia, R.; Rashidi, M., Cyclometalated Cluster Complex with a Butterfly-Shaped Pt_2Ag_2 Core. *Inorg Chem* **2010**, *49*, 2721-2726.
24. Forniés, J.; Sicilia, V.; Casas, J. M.; Martín, A.; López, J. A.; Larraz, C.; Borja, P.; Ovejero, C., Pt-Ag Clusters and their Neutral Mononuclear Pt(II) Starting Complexes: Structural and Luminescence Studies. *Dalton Trans.* **2011,** *40*, 2898-2912.
25. Baya, M.; Belío, U.; Fernández, I.; Fuertes, S.; Martín, A., Unusual Metal-Metal Bonding in a Dinuclear Pt-Au Complex: Snapshot of a Transmetalation Process. *Angew. Chem. Int. Ed.* **2016**, *55*, 6978-6982.
26. Baya, M.; Belío, U.; Campillo, D.; Fernandez, I.; Fuertes, S.; Martín, A., Pt-M Complexes (M=Ag, Au) as Models for Intermediates in Transmetalation Processes. *Chem. Eur. J.* **2018**, *24*, 13879-13889.
27. Yamaguchi, T.; Yamazaki, F.; Ito, T., The First Examples of Platinum(II)−Cadmium(II) Bonds: The Role of Strong Field Ligands in Making Dative Pt→M Bonds. *J. Am. Chem. Soc.* **1999**, *121*, 7405-7406.
28. Forniés, J.; Ibáñez, S.; Martín, A.; Gil, B.; Lalinde, E.; Moreno, M. T., Synthesis, Characterization, and Optical Properties of Pentafluorophenyl Complexes with a Pt-Cd Bond. *Organometallics* **2004**, *23*, 3963-3975.
29. Berenguer, J. R.; Gil, B.; Fernández, J.; Forniés, J.; Lalinde, E., Self-Assembly of Luminescent Alkynyl-Based Platinum-Cadmium Complexes Containing Auxiliary Diimine or Terpyridine Ligands. *Inorg Chem* **2009,** *48*, 5250-5262.
30. Ara, I.; Forniés, J.; Sicilia, V.; Villarroya, P. Synthesis and Characterisation of New Binuclear Complexes Containing a Relatively Strong Pt to Hg Donor Bond. Molecular Structure of Complex $[Pt(C\hat{}P)(\mu\text{-}O_2CCH_3)_2Hg(O_2CCH_3)]$ *Dalton Trans* **2003**, 4238-4244.

31. Forniés, J.; Martín, A.; Sicilia, V.; Villarroya, P.,Reactivity of [M(C∧P)(S_2CNMe_2)] [M = Pt, Pd; C∧P = CH_2−C_6H_4−P(*o*-tolyl)$_2$-κ*C*,*P*] toward Mercury(II) Carboxylates. X-ray Molecular Structures of [Pt(C∧P)(S_2CNMe_2)(O_2CCF_3)Hg(O_2CCF_3)] and [Pd(S_2CNMe_2){μ-P(*o*-tolyl)$_2$−C_6H_4−CH_2−}(μ-O_2CCH_3)Hg(O_2CCH_3)] *Organometallics* **2000**, *19*, 1107-1114.
32. Nagle, J. K.; Balch, A. L.; Olmstead, M. M., $Tl_2Pt(CN)_4$: a non-columnar, luminescent form of $Pt(CN)_4^{2-}$ containing platinum-thallium bonds, 110, 319. *J. Am. Chem. Soc.* **1988**, *110*, 319-321.
33. Usón, R.; Forniés, J.; Tomás, M.; Garde, R.; Merino, R. I., Synthesis of Heteronuclear Pt−Tl Complexes with Donor−Acceptor Bonds. X-ray Structures of cis-[Tl(μ2-$OOCCH_3$)Pt(PPh_3)(C_6F_5)$_2$] and (NBu_4)$_2$[{Pt(C_6F_5)$_3$}$_2${(μ2-O,μ3-O'CCH_3)Tl}$_2$]. *Inorg. Chem.* **1997**, *36*, 1383-1387.
34. Berenguer, J. R.; Lalinde, E.; Martín, A.; Moreno, M. T.; Sanchez, S.; Shahsavari, H. R., Binuclear Complexes and Extended Chains Featuring Pt^{II}-Tl^{I} Bonds: Influence of the Pyridine-2-Thiolate and Cyclometalated Ligands on the Self-Assembly and Luminescent Behavior. *Inorg. Chem.* **2016,** *55*, 7866-7878.
35. Jamali, S.; Ghazfar, R.; Lalinde, E.; Jamshidi, Z.; Samouei, H.; Shahsavari, H. R.; Moreno, M. T.; Escudero-Adán, E.; Benet-Buchholz, J.; Milic, D., Cyclometalated heteronuclear Pt/Ag and Pt/Tl complexes: a structural and photophysical study. *Dalton Trans.* **2014,** *43*, 1105.
36. Stork, J. R.; Olmstead, M. M.; Balch, A. L., ~~J. Am. Chem. Soc. 2005, 127, 6512~~. *J. Am. Chem. Soc.* **2005**, *127*, 6512-6513.
37. Fuertes, S.; Chueca, A. J.; Martín, A.; Sicilia, V., Pt_2Tl Building Blocks for Two-Dimensional Extended Solids: Synthesis, Crystal Structures, and Luminescence. *Cryst. Growth Des.* **2017**, *17*, 4336-4346.
38. Forniés, J.; García, A.; Lalinde, E.; Moreno, M. T., Luminescent One- And Two-Dimensional Extended Structures and a Loosely Associated Dimer Based on Platinum(II)–Thallium(I) Backbones. *Inorg. Chem.* **2008,** *47*, 3651-3660.
39. Forniés, J.; Fuertes, S.; Martín, A.; Sicilia, V.; Gil, B.; Lalinde, E., Extended Structures Containing Pt(II)–Tl(I) Bonds. Effect of these Interactions on the Luminescence of Cyclometalated Pt(II) Compounds. *Dalton Trans.* **2009**, 2224-2234.
40. Belio, U.; Fuertes, S.; Martin, A., Preparation of Pt-Tl Clusters Showing New Geometries. X-ray, NMR and Luminescence Studies. *Dalton Trans.* **2014,** *43*, 10828-10843.
41. Forniés, J.; Giménez, N.; Ibáñez, S.; Lalinde, E.; Martín, A.; Moreno, M. T., An Extended Chain and Trinuclear Complexes Based on Pt(II)−M (M = Tl(I), Pb(II)) Bonds: Contrasting Photophysical Behavior. *Inorg. Chem.* **2015,** *54*, 4351-4363 and references therein.
42. Balch, A. L.; Fung, E. Y.; Nagle, J. K.; Olmstead, M. M.; Rowley, S. P., Pb(II)/Pt(II) Complexes with and without Pb-Pt Interactions. *Inorg. Chem.* **1993,** *32*, 3295-3299.
43. Casas, J. M.; Forniés, J.; Martín, A.; Orera, V. M.; Orpen, A. G.; Rueda, A. J., Synthesis, Structural Characterization, and Spectroscopic Studies of Heterodimetallic [NBu_4][(C_6F_5)$_3$Pt(μ-Pb)(μ-X)Pt(C_6F_5)$_3$] (X= Cl, OH) Complexes. *Inorg. Chem.* **1995,** *34*, 6514-6519.
44. Sicilia, V.; Forniés, J.; Fuertes, S.; Martín, A., New Dicyano Cyclometalated Compounds Containing Pd(II)−Tl(I) Bonds as Building Blocks in 2D Extended Structures: Synthesis, Structure, and Luminescence Studies. *Inorg. Chem.* **2012,** *51*, 10581-10589.
45. Sajoto, T.; Djurovich, P. I.; Tamayo, A.; Yousufuddin, M.; Bau, R.; Thompson, M. E.; Holmes, R. J.; Forrest, S. R., Blue and Near-UV Phosphorescence from Iridium Complexes with Cyclometalated Pyrazolyl or N-Heterocyclic Carbene Ligands *Inorg. Chem.* **2005,** *44*, 7992-8003.

46. Poma, A.; Forni, A.; Baldoli, C.; Mussini, P. R.; Bossi, A., Cyclometalated Pt(II) Complexes with a Bidentate Schiff-Base Ligand Displaying Unexpected cis/trans Isomerism: Synthesis, Structures and Electronic Properties. *Dalton Trans.* **2017**, *46*, 12500-12506.
47. Develay, S.; Blackburn, O.; Thompson, A. L.; Williams, J. A. G., Cyclometalated Platinum(II) Complexes of Pyrazole-Based, NΛCΛN-Coordinating, Terdentate Ligands: the Contrasting Influence of Pyrazolyl and Pyridyl Rings on Luminescence. *Inorg. Chem.* **2008**, *47*, 11129-11142.
48. Vezzu, D. A. K.; Deaton, J. C.; Jones, J. S.; Bartolotti, L.; Harris, C. F.; Marchetti, A. P.; Kondakova, M.; Pike, R. D.; Huo, S., Highly Luminescent Tetradentate Bis-Cyclometalated Platinum Complexes: Design, Synthesis, Structure, Photophysics, and Electroluminescence Application. *Inorg. Chem.* **2010**, *49*, 5107-5119.
49. Nahaei, A.; Rasekh, A.; Rashidi, M.; Hosseini, F. N.; Nabavizadeh, S. M., Phenylpyrazolate Cycloplatinated(II) Complexes: Kinetics of Oxidation to Pt(IV) Complexes. *J Organomet Chem* **2016**, *815-816*, 35-43.
50. Taidakov, I.; Ambrozevich, S.; Saifutyarov, R.; Lyssenko, K.; Avetisov, R.; Mozhevitina, E.; Khomyakov, A.; Khrizanforov, M.; Budnikova, Y.; Avetissov, I., New Pt(II) Complex with Extra Pure Green Emission for OLED Application: Synthesis, Crystal Structure and Spectral Properties. *J Organomet Chem* **2018**, *867*, 253-260.
51. Wu, W. T.; Guo, H. M.; Wu, W. H.; Ji, S. M.; Zhao, J. Z., Long-Lived Room Temperature Deep-Red/Near-IR Emissive Intraligand Triplet Excited State (^{3}IL) of Naphthalimide in Cyclometalated Platinum(II) Complexes and its Application in Upconversion. *Inorg. Chem.* **2011**, *50*, 11446-11460.
52. Batagoda, B. K. T.; Djurovich, P. I.; Brase, S.; Thompson, M. E., Synthesis and Characterization of Phosphorescent Cyclometalated Ir and Pt Heteroleptic Complexes Using Cyclophane-Based Chelates. *Polyhedron* **2016**, *116*, 182-188.
53. Fuertes, S.; Chueca, A. J.; Perálvarez, M.; Borja, P.; Torrell, M.; Carreras, J.; Sicilia, V., White Light Emission from Planar Remote Phosphor Based on NHC Cycloplatinated Complexes. *ACS App. Mat. Interfaces* **2016,** *8*, 16160-16169.
54. Fuertes, S.; García, H.; Perálvarez, M.; Hertog, W.; Carreras, J.; Sicilia, V., Stepwise Strategy to Cyclometallated Pt^{II} Complexes with N-Heterocyclic Carbene Ligands: A Luminescence Study on New β-Diketonate Complexes. *Chem. - Eur. J.* **2015,** *21*, 1620-1631.
55. Fuertes, S.; Chueca, A.; Arnal, L.; Martín, A.; Giovanella, U.; Botta, C.; Sicilia, V., Heteroleptic NHC Cycloplatinated Complexes: a New Approach to Highly Efficient Blue-Light Emitters. *Inorg. Chem.* **2017,** *56*, 4829-4839.
56. Sicilia, V.; Fuertes, S.; Chueca, A. J.; Arnal, L.; Martín, A.; Perálvarez, M.; Botta, C.; Giovanella, U., Highly Efficient Platinum-Based Emitters for Warm White Light Emitting Diodes. *J. Mater. Chem. C* **2019,** *7*, 4509-4516.
57. Ogawa, T.; Sameera, W. M. C.; Saito, D.; Yoshida, M.; Kobayashi, A.; Kato, M., Phosphorescence Properties of Discrete Platinum(II) Complex Anions Bearing N-Heterocyclic Carbenes in the Solid State. *Inorg.Chem.* **2018,** *57*, 14086-14096.
58. Sicilia, V.; Fuertes, S.; Martín, A.; Palacios, A., N-Assisted C-Ph-H Activation in 3,8-Dinitro-6-phenylphenanthridine. New C,N-Cyclometalated Compounds of Platinum(II): Synthesis, Structure, and Luminescence Studies. *Organometallics* **2013,** *32*, 4092-4102.
59. Forniés, J.; Sicilia, V.; Larraz, C.; Camerano, J. A.; Martín, A.; Casas, J. M.; Tsipis, A. C., One-Pot and Step-by-Step N-Assisted C-Ph-H Activation in 2-(4-Bromophenyl)imidazol[1,2-

a]pyridine: Synthesis of a New C,N-Cyclometalated Compound [{Pt(C^N)(μ-Cl)}$_2$] as Precursor of Luminescent Platinum(II) Compounds. *Organometallics* **2010**, *29*, 1396-1405.
60. Mabbott, D. J.; Mann, B. E.; Maitlis, P. M., Cationic (η^3-allylic) (η^4-diene)-palladium and -platinum complexes. *J. Chem. Soc., Dalton Trans.* **1977**, 294-299.
61. Mann, B. E.; Shaw, B. L.; Shaw, G., Transition metal-carbon bonds. Part XXVI. Allylic and olefin complexes of platinum(II). *J. Chem. Soc.Inorg. Phys. Theor* **1971**, 3536-3544.
62. Díez, A.; Forniés, J.; Larraz, C.; Lalinde, E.; López, J. A.; Martín, A.; Moreno, M. T.; Sicilia, V., Structural and Luminescence Studies on π···π and Pt···Pt Interactions in Mixed Chloro-lsocyanide Cyclometalated Platinum(II) Complexes. *Inorg. Chem.* **2010**, *49*, 3239-3251.
63. Otto, S.; Samuleev, P. V.; Polyakov, V. A.; Ryabov, A. D.; Elding, L. I., Pseudo-rotation Mechanism for Fast Olefin Exchange and Substitution Processes at Orthometalated C,N-Complexes of Platinum(II). *Dalton Trans.* **2004**, 3662-3668.
64. Dehand, J.; Pfeffer, M., Cyclometallated Compounds. *Coord. Chem. Rev.* **1976**, *18*, 327-352.
65. Fuertes, S.; Chueca, A. J.; Martín, A.; Sicilia, V., New NHC Cycloplatinated Compounds. Significance of the Cyclometalated Group on the Electronic and Emitting Properties of bis-cyanide Compounds. *J. Organomet. Chem.* **2019**, *889*, 53-61.
66. Rausch, A. F.; Monkowius, U. V.; Zabel, M.; Yersin, H., Bright Sky-Blue Phosphorescence of [n-Bu$_4$N][Pt(4,6-dFppy)(CN)$_2$]: Synthesis, Crystal Structure, and Detailed Photophysical Studies. *Inorg. Chem.* **2010**, *49*, 7818-7825.
67. Forniés, J.; Fuertes, S.; Larraz, C.; Martín, A.; Sicilia, V.; Tsipis, A. C., Synthesis and Characterization of the Double Salts [Pt(bzq)(CNR)$_2$][Pt(bzq)(CN)$_2$] with Significant Pt···Pt and π···π Interactions. Mechanistic Insights into the Ligand Exchange Process from Joint Experimental and DFT Study. *Organometallics* **2012**, *31*, 2729-2740.
68. Belío, U.; Fuertes, S.; Martín, A., Synthesis and Characterization of a "Pt$_3$Tl" Cluster Containing an Unprecedented Trigonal Environment for Thallium(I). *Inorg. Chem.* **2013**, *52*, 5627-5629.
69. Tronnier, A.; Pöthig, A.; Metz, S.; Wagenblast, G.; Münster, I.; Strassner, T., Enlarging the π System of Phosphorescent (C^C*) Cyclometalated Platinum(II) NHC Complexes. *Inorg. Chem.* **2014,** *53*, 6346-6356.
70. Buss, C. E.; Mann, K. R., Synthesis and Characterization of Pt(CN-p-(C$_2$H$_5$)C$_6$H$_4$)$_2$(CN)$_2$, a Crystalline Vapoluminescent Compound That Detects Vapor-Phase Aromatic Hydrocarbons. *J. Am. Chem. Soc.* **2002,** *124*, 1031-1039.
71. Caracelli, I.; Haiduc, I.; Zukerman-Schpector, J.; Tiekink, E. R. T., M···π (arene) Interactions for M = gallium, indium and thallium: Influence Upon Supramolecular Self-Assembly and Prevalence in Some Proteins. *Coord. Chem. Rev.* **2014,** *281*, 50-63.
72. Bondi, A., van der Waals Volumes and Radii *J. Phys. Chem.* **1964,** *68*, 441-451.
73. Fernández, J.; Forniés, J.; Gil, B.; Gómez, J.; Lalinde, E.; Moreno, M. T., Synthesis, Structures, and Luminescence Behavior of Mixed Metal Alkynyl Platinum-Cadmium Complexes. *Organometallics* **2006,** *25*, 2274-2283.

For use in the table of contents

Anionic bis-cyanide complexes $NBu_4[Pt(Naph^E)(CN)_2]$ containing a cyclometalated naphthyl moeity bearing pyrazole (**4A**) and carbene (**4B**) as neutral fragments react with $TlPF_6$ to render metal-metal bonded Pt-Tl complexes. They show different extended structures and photophysical properties depending only on the neutral motif (pyrazole or carbene).